DROPLET-LIKE BENT MULTIMODE FIBER SENSOR FOR TEMPERATURE AND REFRACTIVE INDEX MEASUREMENT

N. Sidek[1], A. I. Azmi[1], M. A. A. Razak[2], M. R. Salim[1], A. S. Abdullah[1] and M. Y. Mohd Noor[1]
[1]Communication Engineering Department, Faculty of Electrical Engineering, Universiti Teknologi Malaysia, Johor, Malaysia
[2]Electronic and Computer Engineering Department, Faculty of Electrical Engineering, Universiti Teknologi Malaysia, Johor, Malaysia
E-Mail: asrul@utm.my

ABSTRACT

This work proposes and demonstrates a bent multimode interference (MMI) sensor for refractive index and temperature measurement. The MMI structure was fabricated by successive splicing between single-mode-multimode-single-mode (SMS) fibers. A droplet-like bent was introduced in the multimode fiber section for excitation of modes into the acrylate coating. The excitation of higher modes into the acrylate coating is particularly interesting due high thermo-optic coefficient of acrylate which could improve temperature sensitivity, while evanescent field interaction of modes at the acrylate surface with surrounding material could be used for refractive index sensing. These modes experienced phase changes due to temperature and/or refractive index changes, consequently shift the spectra of the sensor. The sensor structure was simulated using BeamProp software to determine the required bending to excite light into acrylate coating for sensing. In experiment, a 3.5 mm bent sensor demonstrated refractive index sensitivity of 42.41 nm/RIU tested with refractive index between 1.30-1.395. Meanwhile, temperature sensitivity of 1.317nm/˚C was attained using 5 mm bent sensor between 25 °C to 35 °C. The low cost and simple sensor structure is desirable in many applications including for detection, diagnosis, and determine of health, safety, environmental, liquid food, and water quality control.

Keywords: multimode interference, bent fiber, temperature, refractive index, curvature radius.

INTRODUCTION

Fiber optic sensing technology has been tremendously evolved over the last few years to meet demands in various applications. Fiber optic sensors offer interesting features such as lightweight, small size and immunity to electromagnetic interference (EMI), while at the same time deliver the desired performance which comparable to the electronic sensors. Therefore, fiber optic sensor has found its place in various applications for measurement of parameters such as rotation, acceleration, magnetic field, temperature, pressure, acoustic, vibration, strain and refractive index. There are several types of fiber optic sensing techniques that have been developed such as fiber Bragg grating (FBG) [1], fiber interferometer [2] and fiber multimode interference (MMI) structure [3-11]. Recently, fiber MMI sensor gained attention from sensing and communication fields alike. A typical MMI-based optical fiber sensor can be constructed by single mode-multimode-single mode (SMS) fiber structure which provides attractive characteristics such as simple preparation, high sensitivity and good spectral characteristics.

There are different schemes of fiber MMI sensor have been proposed recently. A SMS structure with tapered coreless multimode fiber was reported to have sensitivity of 2946 nm/RIU at index range of 1.42 to 1.43 [3]. In different work a coreless-multimode fiber was used for simultaneous measurement of temperature and refractive index, which demonstrated temperature and refractive index sensitivity of -1.88 nm/˚C and 2800 nm/RIU, respectively [4]. Besides that, a SMS structure with etched multimode fiber section was tested and achieved measurement resolution of 5.3×10^{-5}/RIU [5]. A SMS structure is also possible to be used as temperature sensor with suitable coating or packaging with high thermo-optic material, for example a polymer coated SMS has been reportedly to attain maximum sensitivity of 706 pm/°C [6]. In other research work, a highly sensitive liquid core temperature sensor based on MMI effect was proposed using simple SMS fiber structure and the liquid-core MMF filled with index matching oil with refractive index higher than that of the capillary [7]. The reported temperature sensitivity is the highest for fiber-based MMI temperature sensor with the sensitivity of 20 nm/°C. A possible scheme to improve SMS structure performance without requirement of complex fabrication process is by bending technique. A low temperature sensor based on bent MMI fiber attained temperature sensitivities of -2060 pm/˚C and -25.1 nW/˚C for wavelength and intensity based interrogation, respectively, for low temperature range of 27˚C to 31˚C [8].

Although bent SMS has been demonstrated as feasible sensing technique, there is lack of systematic study on the structure to obtain clear understanding of its operation. Hence, this paper presents theoretical, simulation and experimental works to examine bent SMS and further verify its sensing performance. Theoretical simulation based on BeamProp software is performed to determine the required bending for modes excitation from fiber core into acrylate coating, which would be useful for temperature sensing due to the high thermo-optic coefficient of the acrylate. The bending also makes possible for refractive index sensing via evanescent field interaction with the surrounding material. Experimental works is carried out to determine sensor response due to different curvature radius for temperature and refractive index sensing.

THEORY AND SENSING PRINCIPLE

SMS fiber structures with optimized length have been shown to be sensitive to physical perturbations such as temperature and strain [11]. This is due to the inherent properties of optical fiber that are characterized by the thermal expansion, thermo-optics and elasto-optic coefficients. Furthermore, with careful selection of fiber properties such material, diameter and length, the sensitivity of the MMI sensor could further enhanced towards the desired measurands. The proposed SMS fiber structure works as the similar basis of a MMI sensor which consists of three sections: a lead-in SMF, a bent MMF section and a lead-out SMF, shown in Figure-1.

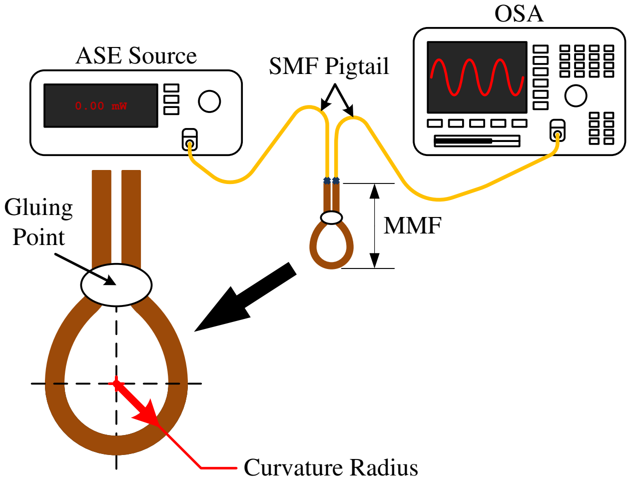

Figure-1. System setup and sensor structure.

When a light enters a straight MMF core, it is divided into a number of eigenmodes (LP_{nm}). Due to the large core diameter, higher order MMF eigenmodes will be also excited, causing interference between different modes as the light field is propagating along the MMF section. As the MMF part is perturbed by temperature or strain changes, higher order modes will experience different phase changes compared with the lower order modes. The interfered modes will be coupled into the lead-out SMF. A straight and a bent MMF are differentiated in terms of refractive index and light field distributions in MMF section. The refractive index and light distributions in the MMF section are not symmetric when the MMF section is bent. Bending causes variation in refractive index of the MMF section due to the elasto-optic effect. When fiber is bent, the inner half of the fiber experienced compression while the outer half experience tension, causes the material refractive index to vary according to the following relation [12]:

$$n_{material} = n\left[1 - \frac{n_0^{\ 2} x}{2R}\left[P_{12} - v(P_{11} + P_{12})\right]\right] \qquad (1)$$

where R is the bent radius, x is the radius of the core/cladding/coating, n_0 is the refractive index of the straight fiber, P_{11} and P_{12} are components of the photo-elastic (or elasto-optical) tensor, and v is Poisson's ratio. The other difference between the bent and straight SMS fiber structure is the propagation path taken by light at the bent fiber section. In a straight fiber, light will propagate only in the core of the MMF, hence MMI only contained within the core. As for bent SMS, at a particular bending radius threshold, higher order MMF eigenmodes can be excited from core into the cladding and further enters into the acrylate coating. Due to the high thermo-optic coefficient of acrylate coating material, any change in surrounding temperature causes a large change to the refractive index of the acrylate. Hence, the high phase change of the modes propagating in the acrylate causes substantial spectra change of the sensor. Bent SMS structure also can be used for refractive index sensing from the exposure of evanescent field to the surrounding media.

All the parameters used in BeamProp simulation are summarized in Table-1.

Table-1. Parameters used in BeamProp simulation.

Parameter	Values
Core diameter	105µm
Cladding diameter	125µm
Acrylate coating diameter	250µm
Length of the curved MMF	π × curvature radius
Curvature radius of the bent	1000µm, 3500µm, 5000µm, 7500µm
Refractive index of core	1.4446
Refractive index of cladding	1.4271
Refractive index of acrylate coating	1.4780

Using the method of conformal transformation, the bent fiber is transformed into a straight fiber with modification of refractive index. The field distributions of the light propagating inside the bent MMF at different radiuses of 1 mm, 3.5 mm, 5 mm and 7.5 mm, and also MMF in straight condition are shown in Figure-2. One particular interest is to know the largest bending radius such that light can be excited into the acrylate coating, such that less tension can be applied without breaking the fiber. As shown in Figure-2(e) for a straight fiber, light is distributed evenly in the fiber core. When a bending radius of 7.5 mm is applied, light field become concentrated at the outer bending surface (right side) but still confined within the core.

However, as the bending radius is decreased to 5 mm, light become available in the coating. For the two smallest radiuses i.e. 1 mm and 3.5 mm, it can be seen clearly light is being transmitted back and forth at the coating-air boundary. The curvature radius size also can influence the higher order eigenmodes to excite out to the coating while most of the lower order modes is lost. The smaller the curvature size, the faster the higher order modes will be reflected out to the coating site. This occur because angle of incident light that reflected in the core is higher than a critical angle cause the light to loss to the cladding and lastly at the coating of the fiber.

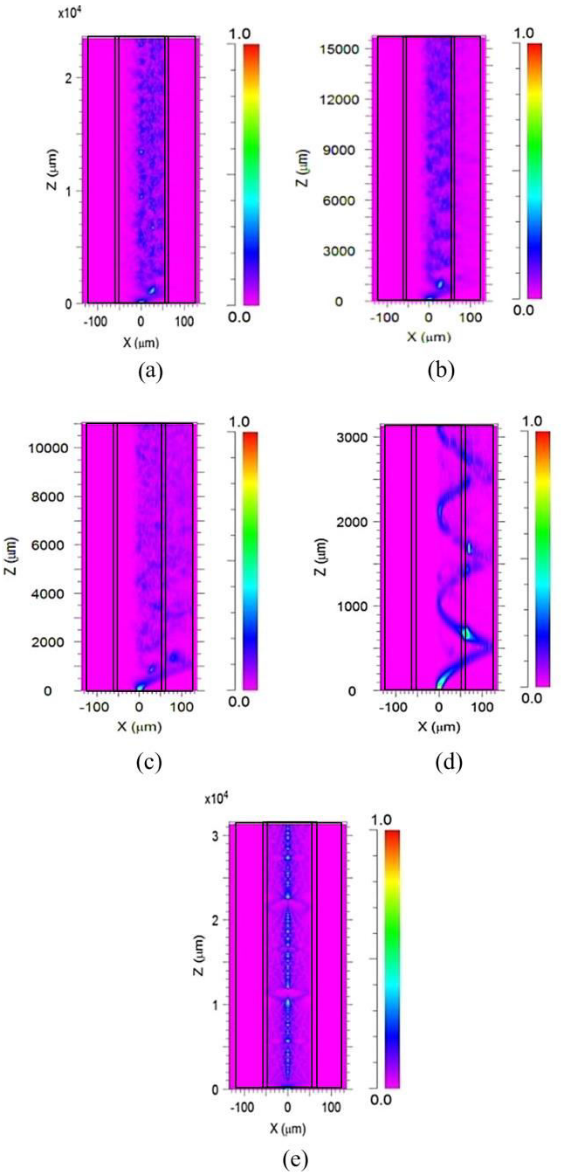

(a) (b)

(c) (d)

(e)

Figure-2. Simulation result of MMF fiberwith (a) curvature radius of 7.5 mm, (b) curvature radius of 5 mm, (c) curvature radius of 3.5 mm, (d) curvature radius of 1.0 mm, and (e) straight condition.

EXPERIMENT RESULT AND DISCUSSIONS

The experimental setup to test the sensor is shown in Figure-1 consists of series connection of a C-band amplified spontaneous emission source (Photonic P-ASE-C-20-NF-F/A), bent-SMS sensor and an optical spectrum analyzer (ANDO AQ6317B). The MMF fiber (Thorlabs FG105LCA) with a core diameter of 105 µm and length 10 cm was spliced between two single mode fiber pigtails. A permanent bending was introduced at midpoint of the MMF section by applying two parts epoxy resin (Selleys Araldite) resulting of a droplet-like shape. Even though, the smaller curvature radius of 1.0 mm would excite more light into acrylate coating, it is practically unfeasible from our testing due to excessive tension which caused fiber breakage at such small bending radius. In experiment work, only sensor with radius 3.5 mm, 5 mm and 7.5 mm were tested. Figure-3 shows the transmission spectra of all the sensors with surrounding RI of 1.30. The sensor with smallest curvature radius of 3.5 mm produced more interference dips due to the fact that the outer part of the coating experience the highest tension due to the smallest bend. Hence, the elasto-optic effect is at the highest with the smallest bent and subsequently more interference pattern will be produced.

Temperature measurement was carried out in water bath (Mermmet) filled with plain water for temperature range from 25°C to 35°C with 1℃ of increment step. The sensor was placed inside the water bath oven but only the tip of the circular sensor head was dipped into the water. RI and temperature sensitivities were measured on the shift of the dip and peak of the wavelength of the transmission spectra. Result for sensor with the highest sensitivity is presented in this section. Figures 4(a) and 4(b) show the transmission spectra and the dip wavelength shift at different temperature for curvature radius of 5 mm. The 5 mm sensor achieved temperature sensitivity up to 1.317 nm/°C for resonant dip at 1555 nm. The sensor also demonstrated good linearity to temperature with R-square value of 0.8899.

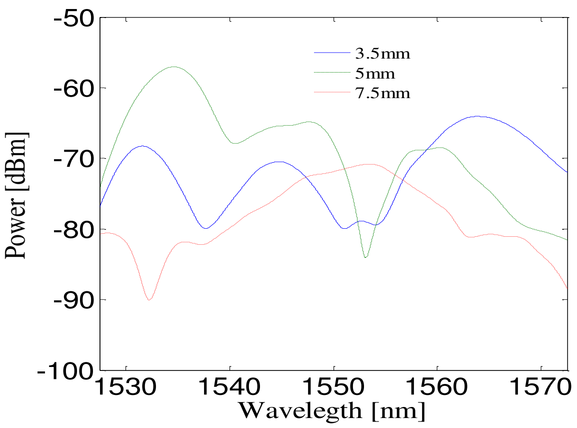

Figure-3. Sensor spectra for different bending radiuses.

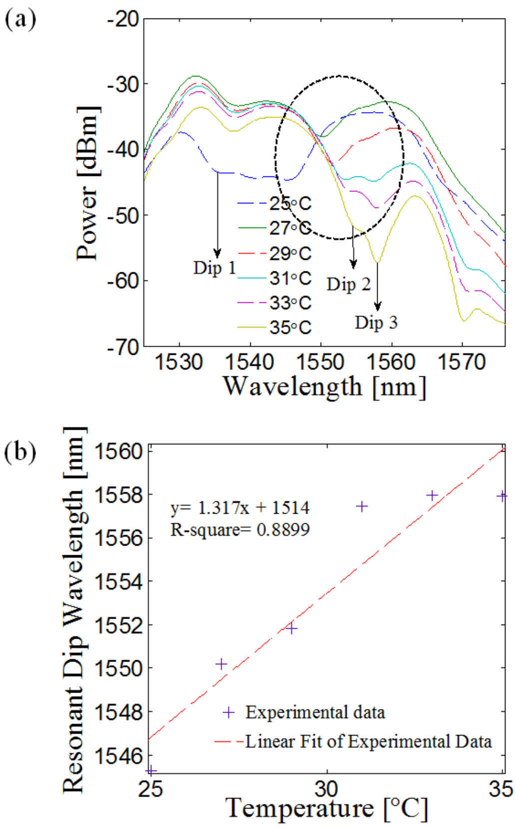

Figure-4. Result for temperature measurement of 5 mm sensor (a) output spectra, and (b) dip wavelength at different temperatures.

Refractive index response was tested by applying series of refractive index liquid (Cargille Series AAA) between 1.3 and 1.395. The oil was applied only at the tip of the sensor head as this part is sensitive to the external RI changes. After the measurement was taken, the tip of the sensor part was clean with distilled water and tissue before it can be tested with other oil refractive index. This step was important in order to make sure that the previous oil used was completely removed from the tested area. Spectra response of sensor with curvature radius of 3.5 mm during RI testing is shown in Figure-5(a). There are three resonant dips at 1538 nm (dip#1), 1548 nm (dip#2) and 1554 nm (dip#3). RI sensitivity of sensor sample at 1554 nm (dip#3) gives the highest sensitivity of 42.41nm/RIU. Figure-5(b) shows the wavelength shift of a dip#3 against RI change in the range of 1.30-1.395. Measurement result for all the tested sensors in temperature and refractive index measurement is summarized in Table-2 and Table-3, respectively.

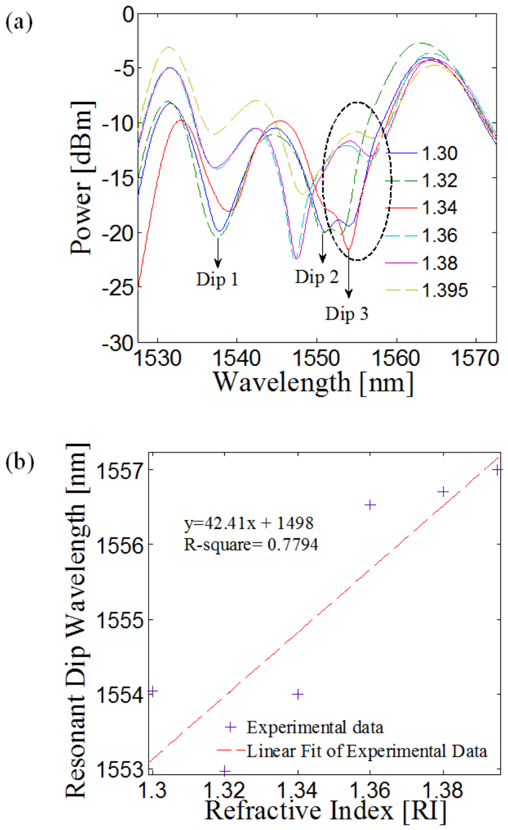

Figure-5. Result for RI measurement of 3.5 mm sensor (a) output spectra, and (b) dip wavelength at different refractive indices.

Table-2. Result for temperature measurement.

Sensor	**Sensitivity** (nm/°C)	**R-square**
3.5mm	-0.1371	0.9606
5mm	1.3170	0.8899
7.5mm	0.1393	0.9417

Table-3. Result for refractive index measurement.

Sensor	**Sensitivity** (nm/RIU)	**R-square**
3.5mm	42.41	0.7794
5mm	-14.99	0.5719
7.5mm	-1.701	0.5200

Based on the obtained result, it is proven that the bent SMS fiber with smaller curvature radius of 3.5 mm gives a higher sensitivity for the refractive index measurement. This is because the smaller the curvature radius of the bent SMS fiber, the stronger the SMS fiber bent, thus the greater the number of higher order MMF eigenmodes will be excited from core to the cladding and across the acrylate coating. Therefore, the sensitivity of the bent SMS fiber sensor will be increased due to the high TOC of acrylate coating. For temperature measurement, the sensor with curvature radius of 5 mm is more sensitive compare to the fiber sensor with smaller curvature radius of 3.5 mm.

CONCLUSIONS

In conclusion, droplet–like bent SMS fiber sensors with different curvature radius of 3.5 mm, 5 mm, and 7.5 mm were studied and experimented for measurement of refractive index and temperature. Compared with bent SMS fiber sensor reported previously, the bent SMS sensor is thoroughly investigated with the variation of size of curvature radius of the bent SMS fiber. From experimental result, the bent SMS fiber with a curvature radius of 3.5 mm achieved maximum of 42.41 nm/RIU for refractive index measurement. While for the temperature measurement, sensor with curvature radius of 5 mm gives a better sensitivity of 1.317 nm/°C. Further investigation is necessary to understand the potential of this type of sensor on other application such as water level application.

ACKNOWLEDGEMENTS

We wish to acknowledge for the support received from the Research University Grants (14J23) by Ministry of Education, Malaysia.

REFERENCES

[1] I. Azmi, D. Sen, W. Sheng, J. Canning and G.-D. Peng. 2011. Performance Enhancement of Vibration Performance Enhancement of Vibration Sensing Employing Multiple Phase-Shifted Fiber Bragg Grating. Journal of Lightwave Technology. 29(22): 3453-3460.

[2] A.I. Azmi, A. S. Abdullah, M. Y. Mohd Noor and *et al.* 2016. Intensity-Modulated Temperature Sensor Based on Fiber Interferometer with Optical Bandpass Filtering. Microwave and Optical Technology Letter. 58(6): 1458-1462.

[3] Claudecir R. Biazoli, Susana Silva, Marcos A. R. Franco, Orlando Frazão, and Cristiano M. B. Cordeiro. 2012. Multimode Interference Tapered Fiber Refractive Index Sensors. Applied Optics. 51(24): 5941-5945.

[4] Susana Silva, Edwin G. P. Pachon, Marcos A. R. Franco, Juliano G. Hayashi, F. Xavier Malcata, Orlando Frazão, Pedro Jorge, and Cristiano M. B. Cordeiro. 2012. Ultrahigh-Sensitivity Temperature Fiber Sensor Based on Multimode Interference. Applied Optics. 51(16): 3236-3242.

[5] Jianfeng Wang, Yongxing Jin, Yu Zhao and Xinyong Dong. 2013. Refractive Index Sensor Based on All-Fiber Multimode Interference. Optik. 124(14): 1845-1848.

[6] L. Xue, Y. Zhang, D. Che, Q. Zhang, L. Yang. 2012. Highly Sensitive Temperature Measurement Based on Polymer-Coated Single-mode, Multimode, Single-mode Fiber Structure. Proc. Of SPIE, 8561.

[7] M.A.F-Fuentes, D. A. May-Aroja, J.R.Guzman-Sepulveda, M. Torres-Cisneros and J.J. Sanchez-Mondragon. 2015. Highly Sensitive Liquid Core Temperature Sensor Based on Multimode Interference Effects. Sensors. 15(10): 26929-26939.

[8] M. Y. Mohd Noor, A. I. Azmi, A.S. Abdullah, A. S. Mohd Supa'at, N. M. Kassim, M. H. Ibrahim, and N. H. Ngajikin. 2015. High Sensitivity of Balloon-Like Bent MMI Fiber Low-Temperature Sensor. Photonics Technology Letter. 27(18): 1989-1992.

[9] J. Huang, X. Lan, A. Kaur, H. Wang, L. Yuan, and H. Xiao. 2014. Temperature Compensated Refractometer Based on a Cascaded SMS/LPFG Fiber Structure. Sensor and Actuators B-Chemical. 198: 384-387.

[10] Wu Q., *et al.* 2011. Experimental Demonstration of a Simple Displacement Sensor Based on a Bent Single-Mode–Multimode–Single-Mode Fiber Structure. Measurement Science and Technology. 22(2):025203.

[11] Aguilar-Soto, J., *et al.* Fiber Optic Temperature Sensor Based on Multimode Interference Effects. Journal of Physics. Conference Series, IOP Publishing.

[12] Schermer R. T. and J. H. Cole. 2007. Improved Bend Loss Formula Verified for Optical Fiber by Simulation and Experiment. IEEE Journal of Quantum Electronics. 43: 899-909.